https://doi.org/10.1016/j.jocs.2018.09.001

Wind Action on Natural Smoke Exhaust in Atria

W.K. Chow*
Research Centre for Fire Engineering
Department of Building Services Engineering
The Hong Kong Polytechnic University
Hong Kong, China

J. Li
Beijing Key Laboratory of Green Built Environment and Energy Efficient Technology
Beijing University of Technology
Beijing, China

*Corresponding author:
Fax: (852) 2765 7198; Tel: (852) 2766 5843
Email: beelize@polyu.edu.hk; bewkchow@polyu.edu.hk
Postal address: Department of Building Services Engineering, The Hong Kong Polytechnic University, Hunghom, Kowloon, Hong Kong.

Submitted: March, 2018
Revised: July, 2018

Abstract

Performance of natural vents installed at height would be affected under strong wind. Smoke might even be pulled downward or inward by wind action if the building is located near to a tall building or on the hillside. The importance of studying aerodynamics around a building located adjacent to a vertical wall while designing static smoke exhaust system will be illustrated in this paper. Air flow pattern around the buildings depends on many factors including wind speed, fire size, height of the vertical wall and distance away from the building, theoretical study is difficult. Numerical simulations with Computational Fluid Dynamics is appropriate to design smoke exhaust system design under these conditions. Key equations of calculating the smoke exhaust rates and the required vent area will be reviewed. Modified equations on smoke exhaust rates with wind effects discussed earlier will be applied.

Keywords: Wind action, Natural vent, Smoke exhaust, Nearby wall

1. Introduction

Smoke exhaust with natural vents, or known as static system, is getting popular [1-6] in large and tall atria in the Far East. Natural venting system is sometimes more preferred because it does not require spaces for housing the fan and duct in the mechanical exhaust system. The associated cost is lower and it might even give better interior appearance. Most natural venting systems consist of horizontal ceiling vents installed on the roof. Many systems are put in cargo terminals where the occupant loading is not high. Therefore, it is more acceptable to the authorities. The driving forces for natural vents [7] are: stack effect due to the difference between temperatures indoors and outdoors, wind-induced action and buoyancy of smoke. In areas with small difference between temperatures indoors and outdoors, stack effect is only significant in tall lift shafts or staircases [8,9]. Wind-induced air flow is a transient phenomenon depending on the conditions of the surroundings. Buoyancy of the hot smoke layer is strong under a big fire. Therefore, buoyancy is the key driving force in removing smoke for natural vents.

However, air motion in areas surrounding an atrium might be fluctuating due to wind action or non-uniform surface thermal heating effects, which are 'thermals'. When sufficiently strong wind is blowing towards the atrium, positive or negative pressure might be induced on the windward and leeward sides. The ceiling vent might become an air intake point rather than an extract point [10,11]. The instanteous vent pressure relative to pressure distribution indoors is a key point. Under extreme conditions, wind will give downward pressure above the vent. This downward wind pressure might be greater than the upward pressure induced by buoyancy. Air pressure distribution inside and outside the atrium should be estimated carefully with reference to the literature results [12-27] in some projects. Therefore, there are concerns on the performance of static smoke exhaust systems, particulary in crowded deep underground subway stations or atrium buildings in high-density tall building areas [1,10,11]. Fire hazard assessment [28] should be reviewed carefully while using static smoke exhaust systems because of the change in pressure distributions around the building due to the nearby tall buildings. The smoke exhaust rates predicted by some empirical equations should be re-evaluated under these conditions.

2. Mass Flow Rate Across the Ceiling Vent

Consider a smoke layer in a naturally ventilated space as in Figure 1. Hydrostatic equations will be used to calculate the variation of pressure within the atrium [13] by taking the cross-sectional area of the atrium is much larger than the area of all openings.

- Insert Figure 1 here -

An atrium fire inducing an axisymmetric plume as in Figure 1 is assumed to have taken place. Take the difference in pressure across the ceiling vent as $P_c - P_{00}$ and that across the inlet as $P_0 - P_A$. The Bernoulli's equation on discharging air through the ceiling vent can be written as:

$$P_c - P_{00} = \frac{1}{2}\rho_g v_c^{\,2} \tag{1}$$

For air entering through the inlet:

$$P_c - P_A = \frac{1}{2}\rho_a v_A^{\,2} \tag{2}$$

The static pressure heads P_{00} and P_c are:

$$P_{00} = P_0 - \rho_a g H \tag{3}$$

$$P_C = P_A - \rho_g g\left(H - H_g\right) - \rho_a g H_g \tag{4}$$

The pressure drop across the ceiling vent caused by the difference in densities of the smoke layer and the surrounding cold air can be given as:

$$\Delta P_o = P_C - P_{00} \tag{5a}$$

Putting in equations (3) and (4), ΔP_o is:

$$\Delta P_o = \left(P_A - P_0\right) + \left(\rho_a - \rho_g\right) g\left(H - H_g\right) \tag{5b}$$

This can be written as:

$$\Delta P_o = \rho_g g'\left(H - H_g\right) - \Delta P_i \tag{5c}$$

where g' represents the reduced gravity due to buoyancy, defined by:

$$g' = \frac{\Delta\rho}{\rho_a} g \tag{6}$$

where $\Delta\rho = \rho_a - \rho_g$

ΔP_C can then be defined as the pressure difference caused by buoyancy ΔP_F and the pressure drop across the inlet vent ΔP_i. That is

$$\Delta P_o = \Delta P_F - \Delta P_i \tag{7}$$

where $\Delta P_F = \rho_g g'(H - H_g)$

Combining equations (5) and equations (1) and (2) gives:

$$\frac{1}{2}\rho_g v_o^{\,2} = P_A - P_0 + \left(\rho_a - \rho_g\right) g\left(H - H_g\right) = \Delta P_F - \frac{1}{2}\rho_a v_i^{\,2} \tag{8}$$

Using mass continuity through the inlet and outlet gives:

$$C_i \rho_a v_i A_A = C_o \rho_g v_o A_C \tag{9}$$

where C_i and C_o refer to the discharge coefficient of inlet and outlet respectively.

Rearranging the above equation,

$$v_i = \frac{C_o \rho_g A_C}{C_i \rho_a A_A} v_o \tag{10}$$

Substituting the expression of the inlet velocity into equation (8), the velocity through the outlet is given by:

$$v_o = \left[\frac{2g\left(\rho_a - \rho_g\right)\left(H - H_g\right)}{\left(1 + \frac{\rho_g C_o{}^2 A_C{}^2}{\rho_a C_i{}^2 A_A{}^2}\right)\rho_g} \right]^{1/2} \tag{11}$$

For incompressible fluid, the mass flow rate through the vent can be obtained by:

$$m_e = C_o \rho_g A_C \left[\frac{2g\left(H - H_g\right)\left(\rho_a - \rho_g\right)}{\left(1 + \frac{\rho_g C_o{}^2 A_C{}^2}{\rho_a C_i{}^2 A_A{}^2}\right)\rho_g} \right]^{1/2} \tag{12}$$

Using the ideal gas law:

$$\rho_a T_a = \rho_g T_g \tag{13}$$

The mass flow rate through the vent can be rewritten as:

$$m_e = C_o \rho_a A_C \left[\frac{2g\left(H - H_g\right)\left(T_g - T_a\right)T_a}{T_g\left(T_g + \frac{T_a C_o{}^2 A_C{}^2}{C_i{}^2 A_A{}^2}\right)} \right]^{1/2} \tag{14}$$

3. Wind Action

Figure 2 shows the flow through the vent under normal condition with the pressure induced by wind of speed v_w. If a similar analysis [2,3] is followed, the ambient pressure outside the inlet vent and outlet vent P_0' and P_{00}' under wind action can be written as:

$$P_0' = C_{wi}\frac{\rho_a v_w^2}{2} + P_0 \tag{15}$$

$$P_{00}' = C_{wo}\frac{\rho_a v_w^2}{2} + P_0 - \rho_a g H \tag{16}$$

C_{wi} represents the outside pressure coefficient at the inlet location, while C_{wo} denotes the outside pressure coefficient at the vent location.

- Insert Figure 2 here -

The hydrostatic equation was applied to study the variation in pressure by assuming the interface of the smoke layer in the atrium is stable under the windy condition. The pressure drop across the ceiling vent $\Delta P_o'$ under wind can be deduced from the equation below:

$$\begin{aligned}\Delta P_o' &= P_A - P_0' + (C_{wi} - C_{wo})\frac{\rho_a v_w^2}{2} + (\rho_a - \rho_g)g(H - H_g) \\ &= \Delta C_w \frac{\rho_a v_w^2}{2} + \rho_g g'(H - H_g) - \Delta P_i'\end{aligned} \tag{17}$$

$\Delta P_i'$ refers to the pressure drop across the inlet vent under the windy condition.

Under windy conditions, it is observed that the vent flow is driven by the pressure difference induced by the combination of buoyancy and wind.

The pressure difference ΔP_w prompted by the wind is:

$$\Delta P_w = (C_{wi} - C_{wo})\frac{\rho_a v_w^2}{2} \tag{18}$$

Putting in equation (17) gives:

$$\Delta P_o' = \Delta P_w + \rho_a g'(H - H_g) - \Delta P_i' \tag{19}$$

Using Bernoulli theorem and considering the flow losses across the inlet and outlet, the velocity v_o' across the outlet vent under wind is given by:

$$v_o' = \left[\frac{(C_{wi} - C_{wo})\rho_a v_w^{\,2} + 2g(\rho_a - \rho_g)(H - H_g)}{\left(1 + \frac{\rho_g C_o^{\,2} A_c^{\,2}}{\rho_a C_i^{\,2} A_A^{\,2}}\right)\rho_g} \right]^{1/2} \tag{20}$$

Combining the ideal gas law with equation (13), the mass flow rate through the vent m_e' of incompressible fluid under wind can be obtained:

$$m_e' = C_o \rho_a A_C \left[\frac{(C_{wi} - C_{wo}) T_g T_a v_w^{\,2} + 2g(H - H_g')(T_g - T_a) T_a}{T_g \left(T_g + \frac{T_a C_o^{\,2} A_C^{\,2}}{C_i^{\,2} A_A^{\,2}} \right)} \right]^{1/2} \tag{21}$$

4. Effect of the Vertical Wall on the Vent Flow

As shown in Figure 2, an atrium with wind blowing from one side is taken as an example. Fire is located at the center of the atrium. The effects of a vertical wall (located on the leeward side) on the smoke vent flow will be discussed.

The CFD software Fire Dynamics Simulator (FDS) version 6.0 [29], developed by the Building and Fire Research Laboratory of the US National Institute of Standards and Technology, is used for numerical studies. The transient conservation equations of mass, momentum, energy, and species for low-speed motion of a gas are solved numerically. The three-dimensional space is divided into rectangular grids in which the gas variables are assumed to be uniform, but changing with time. The Navier-Strokes equations are solved in FDS using large eddy simulation to account for subgrid turbulence. The mixture fraction model is used for combustion reactions. Heat transfer to solid surfaces and convection within the fluid are taken into account. Verification works on applying this FDS to simulate fire-induced smoke transportation and dispersion were reported [30,31]. The predicted results agreed satisfactorily with the experiments, giving justification and confidence for application of FDS in this study.

In order to investigate the effects of the existing vertical wall on the leeward side, the external wind speed and the fire size on the mass vent flow rate through the ceiling vent, three scenarios labeled as S1, S2 and S3 are considered [32]. A constant wind speed is assumed to investigate the effects of wind speed on the top vent flow, as there are different views on using a vertical wind speed profile.

- Scenario S1:
  No vertical wall is constructed at the other side of the building. Different wind speeds of 0 ms^{-1}, 1 ms^{-1}, 3 ms^{-1}, 5 ms^{-1} and 10 ms^{-1} at the same fire size of 3 MW are tested. Three other fire sizes of 1 MW, 5 MW and 10 MW at the same outside wind velocity of 5 ms^{-1} are also simulated.

- Scenario S2:
  A vertical wall is 20 m away from the leeward side of the building. The wall is much higher than the building. Different external wind speeds of 0 ms^{-1}, 1 ms^{-1}, 3 ms^{-1}, 5 ms^{-1} and 10 ms^{-1} are simulated under the same fire power of 3 MW. Different fire powers of 1 MW, 3 MW, 5 MW and 10 MW at the same outside wind velocity of 5 ms^{-1} are studied.

- Scenario S3:
  Different distances of 5 m, 10 m, 20 m and 25 m from the vertical wall to the building are considered, and various external wind speeds of 0 ms^{-1}, 1 ms^{-1}, 3 ms^{-1}, 5 ms^{-1} and 10 ms^{-1} are simulated under the same fire power of 3 MW.

In CFD simulations [12,13], free boundaries have to be handled properly. Therefore, the extended computing domain enclosing the atrium is 61.3 m long, 41.3 m wide and 40.0 m high, as shown in Figure 3. The left boundary is set as inlet boundary, and different inlet wind velocities would be used as shown in scenarios S1 and S2. Other boundaries are set as free boundary.

- Insert Figure 3 here -

In FDS 6.0, for simulations involving buoyant plumes, it is better to assess the quality of the mesh in terms of the non-dimensional parameter $D^*/\delta x$, rather than an absolute mesh size, where D^* is a characteristic fire diameter.

$$D^* = \left(\frac{Q}{\rho_a c_p T_a \sqrt{g}}\right)^{2/5} \tag{22}$$

For the validation study sponsored by the U.S. Nuclear Regulatory Commission, the $D^*/\delta x$ values ranged from 4 to 16 [33]. For the fire size of 1 MW, 3 MW, 5 MW and 10 MW, the relative D^* are 0.96 m, 1.49 m, 1.82 m and 2.4 m. In this study, cells are of size 0.15 m × 0.15 m × 0.15 m used in zone I, as shown in Figure 3(b), and the mesh size of 0.25 m × 0.25 m × 0.25 m is used in the other zones. The ambient temperature is taken as 20 ^oC in all simulations.

5. Numerical Results

With different external wind speeds and different fire sizes for scenarios S1 and S2, the predicted mass vent flow rates are shown in Figures 4 and 5 respectively. It is shown that with the wind speed increasing, the mass exhaust rate will increase under these fire scenarios. With the wind speed increasing, the pressure difference induced by wind between the outlet vent and inlet vent increases, thus giving a higher smoke exhaust rate. When the wind speed is low, say lower than 5 ms^{-1}, the effects of the vertical wall on the leeward side on the mass vent flow rate can be neglected, and the mass vent flow rates are almost the same in the two scenarios. When the wind speed increases beyond 5 ms^{-1}, the mass flow rates in scenario S2 are found to be lower than those in scenario S1. The presence of the leeward vertical wall would reduce the smoke exhaust rate in the atrium. With the wind speed increasing, side wall effects on the pressure distributions around the building will be significant. The pressure difference between the top vent and inlet vent is smaller in scenario S2 compared with that in S1, thus giving a lower smoke exhaust rate. Similar observations can also be found in Figures 6a to 6f.

- Insert Figures 4 to 6 here -

From Figure 5, it can be seen that under the same wind speed action, with the fire size increasing, the mass vent flow will increase, but the increasing rate would be reduced. The mass vent flow in scenario S1 is also found to be higher than that in scenario S2. The vertical wall on the leeward side of the building would reduce the smoke exhaust rate, especially when the fire size is small. When the fire is small, the wind pressure is the main factor for controlling the top vent flow. When the fire size increases, buoyancy effect induced by the hot smoke becomes stronger, both wind pressure and buoyancy contribute to give a higher smoke vent flow. With the buoyancy effect increasing, the effect of wind pressure induced by the side wall on the vent flow becomes less significant. It can be seen in Figure 5 that at large fire size (10 MW), the difference induced by the wall is negligible.

From these figures, it can be found that the vertical wall will change the distribution of wind pressure on the surface of the building. The pressure at the top of the building induced by external wind in scenario S2 is higher than that in scenario S1, although air pressures at the top of the vent in both cases are negative. Due to the presence of the vertical wall, the pressures on the leeward side of the building in scenario S2 are also higher than those in scenario S1. The differences in pressure between the inlet opening and the top vent opening in scenario S1 are larger than those in scenario S2. This gives higher air speed across the vent, hence a higher flow rate across the vent. This can be clearly seen from Figures 7a and 7b.

The difference in transient air pressure ΔP_v between the predicted pressures P_U and P_L at immediately above and below the ceiling vent is given by:

$$\Delta P_v = P_U - P_L \tag{23}$$

Results for ΔP_v are shown in Figure 7a. Values of the transient pressure difference ΔP_v across the ceiling vent in S1 are found to be higher than that in S2. This will give a higher vent flow rate in S1 than that in S2.

Figure 7b shows the wind effects on mass flow rate across the ceiling vent under the fire size of 5 MW for scenarios S1 and S2. The presence of wind can increase the mass flow rate in scenarios without and with the presence of a vertical wall on the leeward side. Comparisons of the mass flow rates calculated by Eq. (21) in which T_g is from the numerical results with those predicted by FDS are shown in Figure 8. It is found that the results calculated using empirical equation (Eq. (21)) are close to the predicted results of FDS. Eq. (21) can thus be used to predict mass exhaust in practice to include the effects of wind and leeward side wall.

- Insert Figure 7 here -

The effect of the distance of vertical wall on the leeward side of the building on the smoke vent flow rate can also be found in Figure 8. It can be seen that the distance of the vertical wall away from the building has large influence on the top vent flow, especially when the external wind speed is large. When the wall is close to the building, say no more than 10 m, the top vent flow increases slightly with the wind speed if the wind speed is not large, but when the wind speed is large (greater than 5 ms^{-1}), the vent flow would decrease compared with that of no wind conditions. The effect of vertical wall on the mass vent flow can be neglected when the wind speed is small for engineering use. When the wall is far away from the building and the wind speed is not large, the effect of the vertical wall on the vent flow could be ignored.

- Insert Figure 8 here -

For the fire size of 3 MW, variations of flow rate across the ceiling vent m_e with a nearby wall distance h_a away to the flow rate across vent m_{eo} without a vertical wall (i.e. free boundary) with the dimensionless distance D/h_a under different wind conditions are shown in Figure 9. As shown in the figure for small D/h_a, ceiling vent flow rate would decrease with the wind speed increasing. Effect of the wind speed on the smoke exhaust rate flow rate is large. With D/h_a increasing, the effect of wind speed on vent flow rate would decrease.

Combining the two effects, when D/h_a is greater than 2.04, little change could be found for the vent flow rate with the wind speed increasing. Effect of the nearby vertical wall on vent flow appears to be small under this condition for this study .

- Insert Figure 9 here -

6. Conclusions

Buoyancy and wind effects on the smoke vent flow across the horizontal ceiling vent of an atrium are studied by theoretical analysis and numerical simulation in this paper. The effect of a wall or a building on the leeward side of the atrium on the performance of the static smoke exhuast system is also disscussed.

The combined effects of wind and buoyancy are the key factors to control the smoke vent flow across the ceiling vent. Presence of a nearby wall or other tall buildings on the leeward side of the atrium would change the wind pressure distributions around the atrium surface. This will largely influence the smoke vent flow when the wind effect is the main factor on the smoke vent flow. The smoke exhaust rate woud be reduced, and the reduction rate would be determined by the side wall distance from the atrium buildings. Effect of adjacent vertical wall on the exhaust rate across the ceiling vent is negligible for long distance away. The critical distance could be estimated by CFD simulations.

For the static smoke exhaust system design in an atrium, empirical equation, e.g. Eq. (21), can be used conveniently. However, the coefficients and variables in the equation are not always obtained easily for the calculation, like the cases in this study. Numerical method should be used to assist the analysis.

Terrains around a building would affect the performance of the static smoke exhuast system. This part should be evaluated carefully while designing static smoke exhaust system for large crowded atria. In addition, meteorological information such as wind speed in different seasons are also important data to consider the the design, for better smoke exhaust performance.

Funding

This work described in this paper was partially supported by a grant from the Research Grants Council of the Hong Kong Special Administrative Region, China for the project “A study on powder explosion hazards and control schemes when clouds of coloured powder are sprayed in partially confined areas” (Project No. PolyU 15252816) with account number B-Q53X, and partially supported by Beijing Natural Science Foundation – Beijing Academy of Science and Technology Joint Funded Project (Grant No: L140002).

Declaration

The authors declare that they have no conflict of interest.

Data Availability

Access to the data used to support the findings of this study will be considered by the author upon request.

Author Biographies

W.K. Chow is the Chair Professor of Architectural Science and Fire Engineering, and Director of Research Centre for Fire Engineering at the Department of Building Services Engineering of The Hong Kong Polytechnic University. He is the Founding President of Society of Fire Protection Engineers (SFPE) – Hong Kong Chapter since 2002; President of the Asia-Oceania Association for Fire Science and Technology since 2007; and Chair of Asia-Oceania Chapters Coordinating Group, SFPE since 2015. He was elected to the SFPE Board of Directors from 2016 to 2019.

Li Junmei is an Associate Professor at the Beijing University of Technology. She is a member of China Fire Protection Association and a fellow member of Chinese Association of Refrigeration. Her research interests include fire safety management in atrium buildings, thermal dynamics of hot gas induced by fire in urban traffic tunnels and Energy saving in buildings.

References

[1] W.K. Chow, Static smoke exhaust in big halls with high occupancy. Department of Building Services Engineering, The Hong Kong Polytechnic University, Hong Kong, 2011. Available at: http://www.bse.polyu.edu.hk/researchCentre/Fire_Engineering/Hot_Issues.html

[2] W.K. Chow, J. Li, Wind effects on performance of static smoke exhaust systems: Horizontal ceiling vents. ASHRAE Transactions, 110, Part 2: 479-488, 2004.

[3] C.L. Chow, J. Li, An analytical model on static smoke exhaust in atria. Journal of Civil Engineering and Management, 16(3): 372-381, 2010.

[4] W.K. Chow, Y. Gao, J.L. Wang, Y.Z. Yang, Effects of wind, buoyancy and thermal expansion on a room fire with natural ventilation. Building and Environment, 82: 420-430, 2014.

[5] W.K. Chow, Y. Gao, J.H. Zhao, J.F. Dang, N.C.L. Chow, A study on tilted tunnel fire under natural ventilation. Fire Safety Journal, 81: 44-57, 2016.

[6] Y. Gao, W.K. Chow, Onsetting internal fire whirls in a room with ceiling vents. Journal of Applied Fire Science, 20(2): 149-165, 2010-2011.

[7] J.H. Klote, J.A. Milke, Design of smoke management systems. ASHRAE Publ. 90022, American Society of Heating, Refrigerating and Air-Conditioning Engineers, Atlanta, USA, 1992.

[8] W.K. Chow, J.H. Zhao, Scale modeling studies on stack effect in tall vertical shafts. Journal of Fire Sciences, 29(6): 531-542, 2011.

[9] W.Y. Hung, W.K. Chow, A review on architectural aspects of atrium buildings. Architectural Science Review, 44(3): 285-295, 2001.

[10] W.K. Chow, Wind environment for a high-rise building adjacent to a vertical wall. Keynote speech presented at the International Conference on Sustainable Development in Building and Environment, SET2 (Sustainable Energy Technology), 24-27 October 2003, Chongqing, China; and appeared also in Journal of Chongqing University (English Edition), Vol. 2, Special Issue, October 2003, pp. 19-25.

[11] W.K. Chow, Wind-induced indoor-air flow in a high-rise building adjacent to a vertical wall. Applied Energy, 77(2): 225-234, 2004.

[12] W.K. Chow, N. Cai, Numerical studies on heat release rate in room fire on liquid fuel under different ventilation factors. International Journal of Chemical Engineering, Volume 2012, Article ID 910869, 13 pages, 2012.

[13] C.L. Chow, W.K. Chow, A brief review on applying computational fluid dynamics in building fire hazard assessment, in: Ingmar Søgaard, Hans Krogh (Eds.), Fire Safety, Nova Science Publishers, 2009.

[14] W.K. Chow, J. Li, Simulation on natural smoke filling in atrium with a balcony spill plume. Journal of Fire Sciences, 19(4): 258-283, 2001.

[15] G.O. Hansell, H.P. Morgan, Design approaches for smoke control in atrium buildings. Building Research Establishment Report BR258, Building Research Establishment, Garston, UK, 1994.

[16] H. Ingason, B. Persson, Effects of wind on natural fire vents. Brandforsk Project 055-921, Swedish National Testing and Research Institute, Fire Technology, SP Report 1995:04, Boras, Sweden, 1995.

[17] B.S. Kandola, Effects of atmospheric wind on flows through natural convection roof vents. Fire Technology, 26(2): 106-120, 1990.

[18] E.W. Marchant, Effect of wind on smoke movement and smoke control systems. Fire Safety Journal, 7: 55-63, 1984.

[19] H.P. Morgan, B.K. Ghosh, G. Garrad, Design methodologies for smoke and heat exhaust ventilation. Building Research Establishment Report BR368, Building Research Establishment, Garston, UK, 1999.

[20] National Fire Protection Association, NFPA 92 Standard for Smoke Control Systems. Quincy, MA, USA, 2012.

[21] M. Poreh, S. Trebukov, Wind effect on smoke motion in building. Fire Safety Journal, 35: 257-273, 2000.

[22] C.F. Than, Smoke venting by gravity roof ventilators under windy conditions. Journal of Fire Protecting Engineering, 4(1): 1-4, 1992.

[23] W.K. Chow, Y. Gao, Oscillating behaviour of fire-induced air flow through a ceiling vent. Applied Thermal Engineering, 29(16): 3289-3298, 2009.

[24] W.K. Chow, Y. Gao, Buoyancy and inertial force on oscillations of thermal-induced convective flow across a vent. Building and Environment, 46(2): 315-323, 2011.

[25] B. Gera, P.K. Sharma, R.K. Singh, Effect of the opening aspect ratio on a buoyant pulsating exchange flow through a circular ceiling opening in a horizontal partition. Heat Transfer – Asian Research, 41(8): 666-680, 2012.

[26] R. Harish, K. Venkatasubbaiah, Numerical simulation of turbulent plume spread in ceiling vented enclosure. European Journal of Mechanics B/Fluids, 42: 142-158, 2013.

[27] R. Harish, K. Venkatasubbaiah, Effects of buoyancy induced roof ventilation systems for smoke removal in tunnel fires. Tunnelling and Underground Space Technology, 42: 195-205, 2014.

[28] W.K. Chow, Performance-based approach to determining fire safety provisions for buildings in the Asia-Oceania Regions, Building and Environment - Fifty Year Anniversary for Building and Environment, 91: 127-137, 2015.

[29] K McGrattan, S. Hostikka,R. McDermott, J. Floyd, C. Weinschenk, K. Overholt, Fire Dynamics Simulator (Version 6.0) User's Guide. NIST Special Publication 1019, National Institute of Standards and Technology, US Department of Commerce, 2013.

[30] K. McGrattan, S. Hostikka,R. McDermott, J. Floyd, C. Weinschenk, K. Overholt, Fire Dynamics Simulator (Version 6.0) Technical Reference Guide, Volume 2: Verification. NIST Special Publication 1018, National Institute of Standards and Technology, US Department of Commerce, 2013.

[31] K. McGrattan, R. McDermott, C. Weinschenk, K. Overholt, S. Hostikka, J. Floyd, Fire Dynamics Simulator (Version 6.0) Technical Reference Guide, Volume 3: Validation. NIST Special Publication 1018, National Institute of Standards and Technology, US Department of Commerce, 2013.

[32] W.K. Chow, J. Li, Wind effect on smoke exhaust by natural vent. Paper presented at 2012 International Coference on Advances in Wind and Structures (AWAS'12), 26-30 August 2012, Seoul, Korea.

[33] K. Hill, J. Dreisbach, F. Joglar, K. Najafi, K. McGrattan, R. Peacock, and A. Hamins, Verification and Validation of selected fire models for nuclear power plant applications. NuREG 1824, United States Nuclear Regulator Commission, Washington DC, 2007.

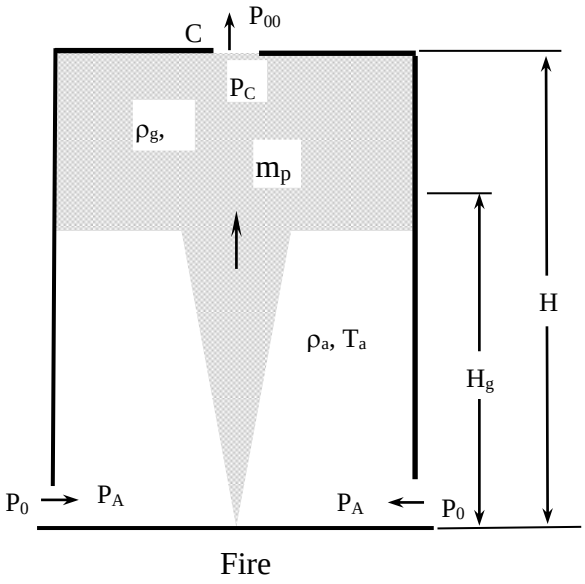

Figure 1: Geometry of the problem for an axisymmetric plume

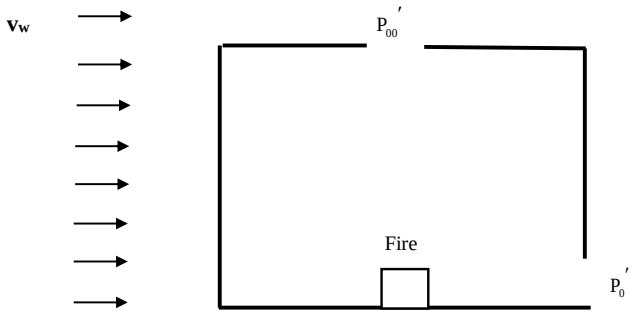

(a) Case S1

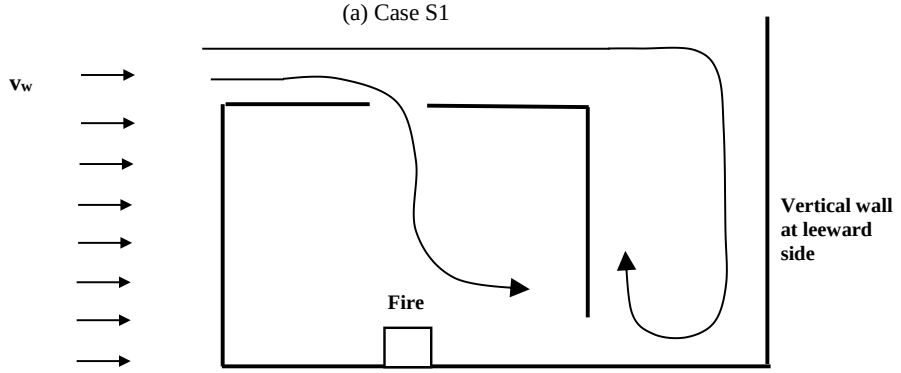

(b) Case S2

Figure 2: Wind effect

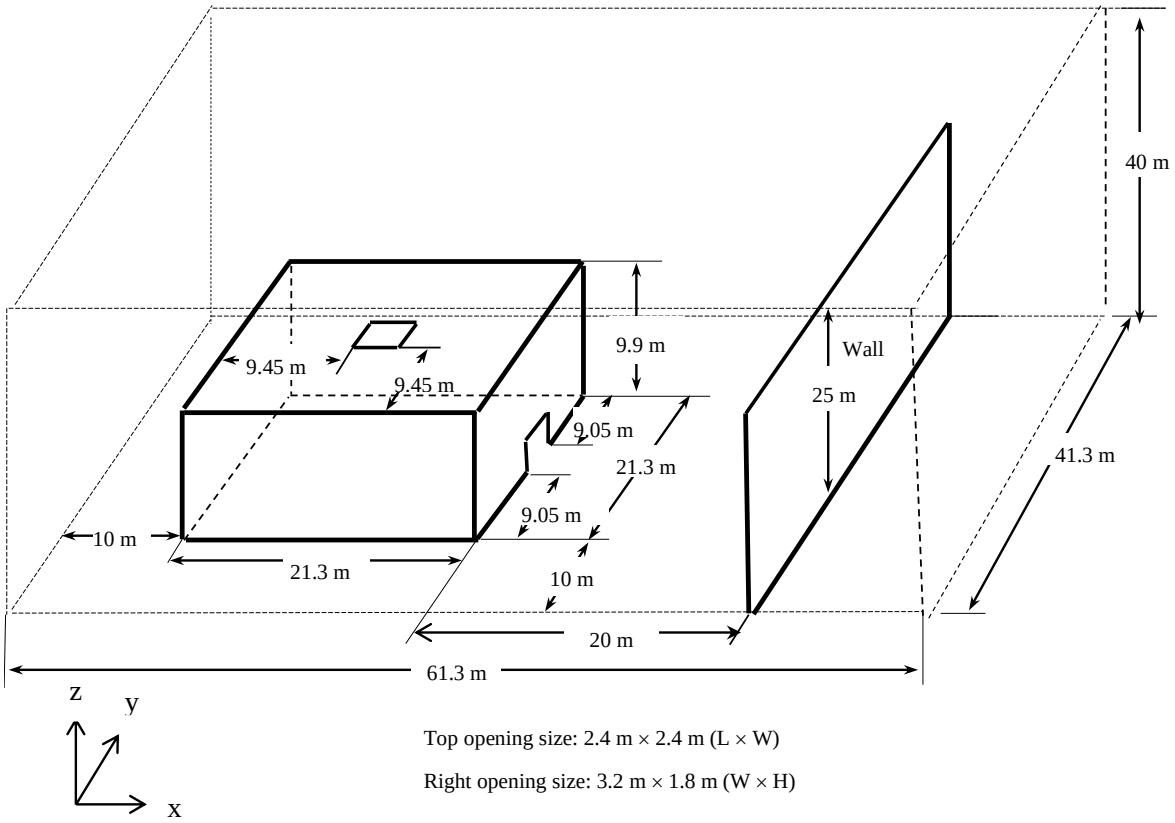

a) Geometry of the atrium and computation domain

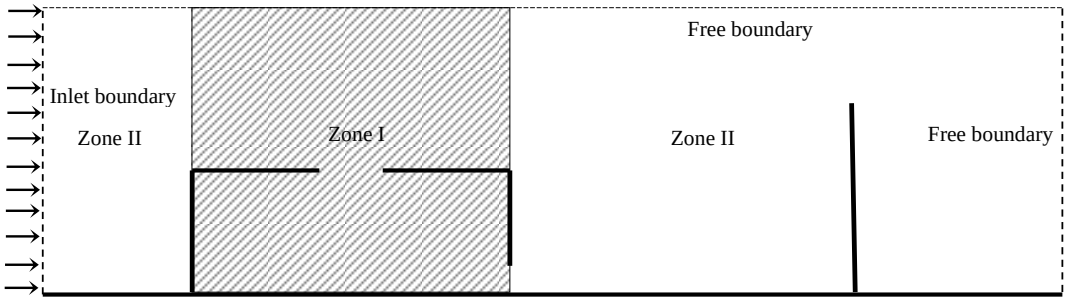

b) Computation zones and boundaries

Figure 3: Geometry of the atrium and computation zone

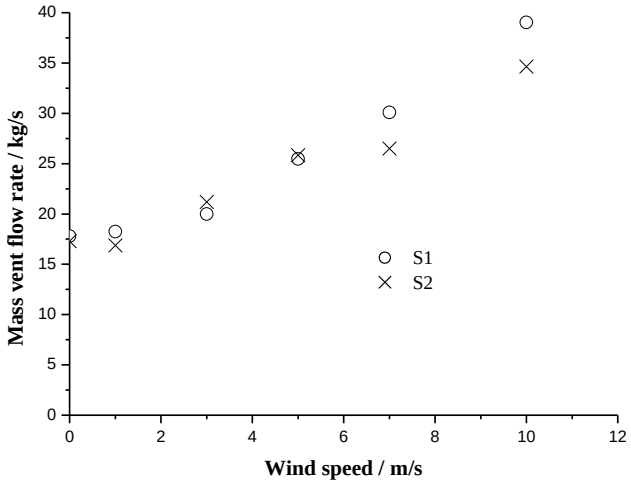

Figure 4: Variation of the vent mass flow rates with wind speeds at 3 MW fire

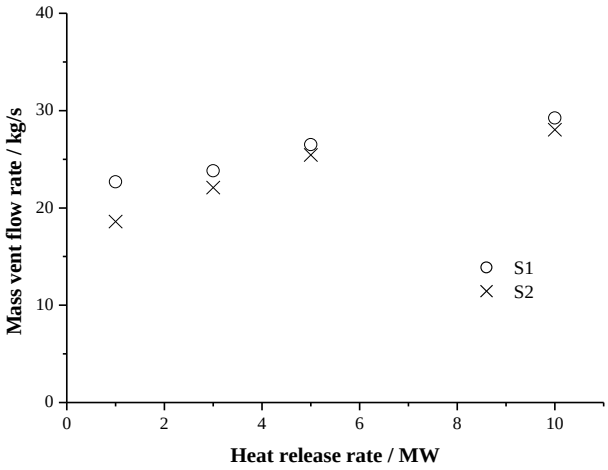

Figure 5: Variation of the vent mass flow rates with fire sizes at 5 ms^{-1} wind speed

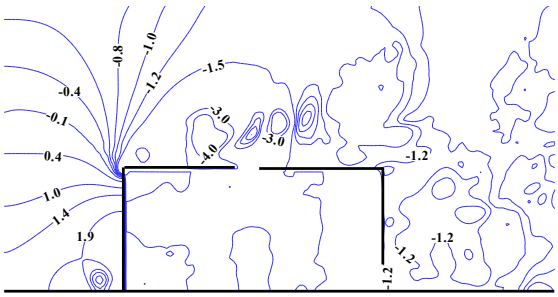

(a) Scenario S1 without fire with wind speed of 5 ms^{-1}

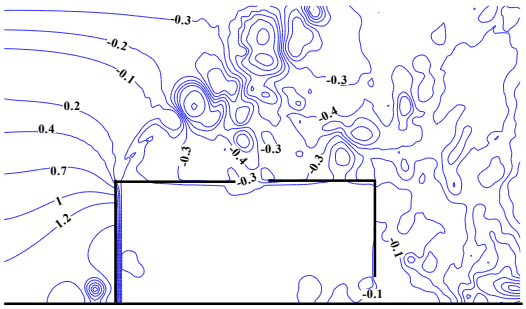

(b) Scenario S2 without fire with wind speed of 5 ms^{-1}

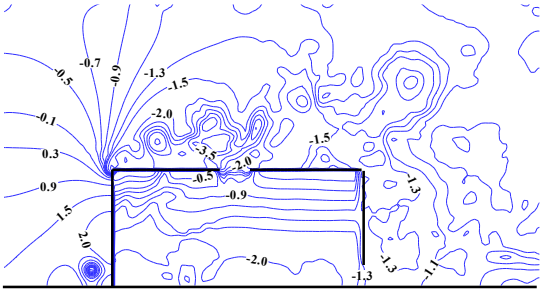

(c) Scenario S1 under a 5 MW fire with wind speed of 5 ms^{-1}

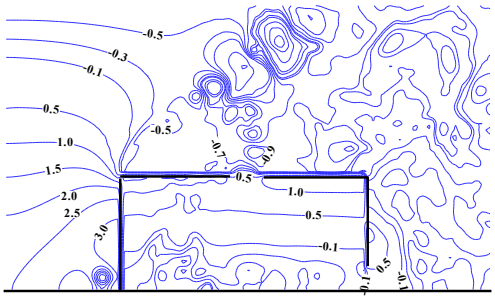

(d) Scenario S2 under a 5 MW fire with wind speed of 5 ms^{-1}

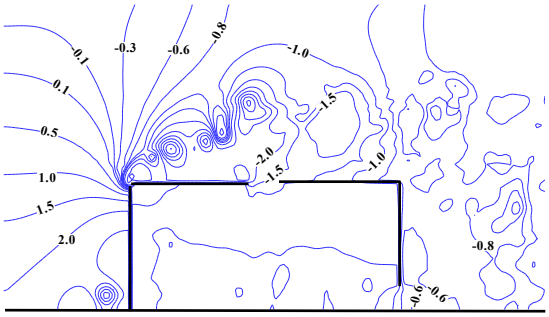

(e) Scenario S1 under a 5 MW fire with wind speed of 10 ms^{-1}

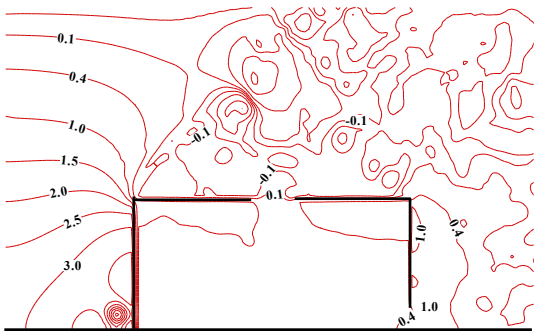

(f) Scenario S2 under a 5 MW fire with wind speed of 10 ms^{-1}

Figure 6: Numerical pressure distribution

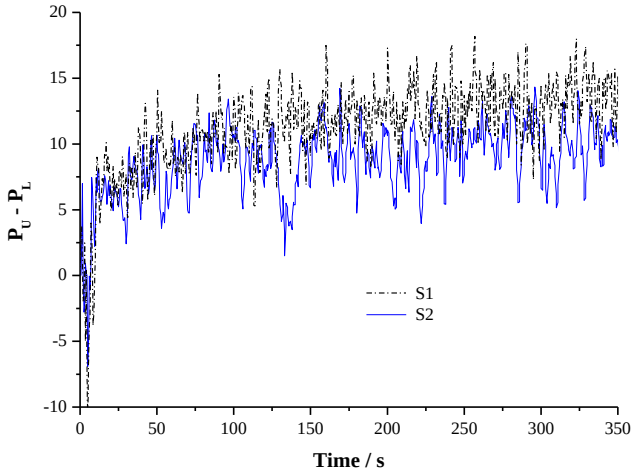

(a) Numerical transient pressure difference across the ceiling vent

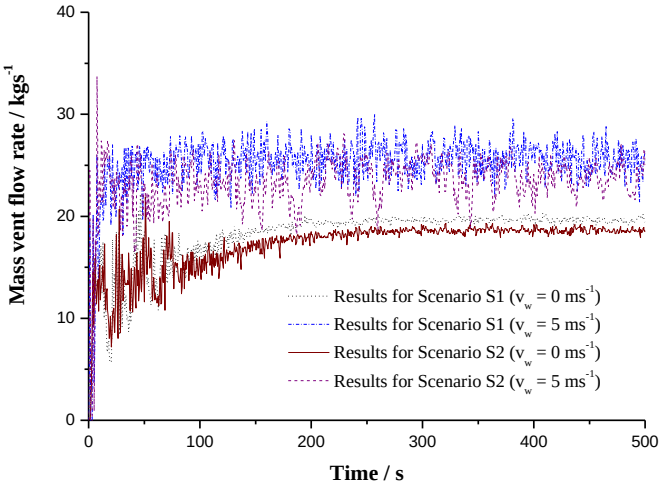

(b) Mass vent flow rates across the ceiling vent

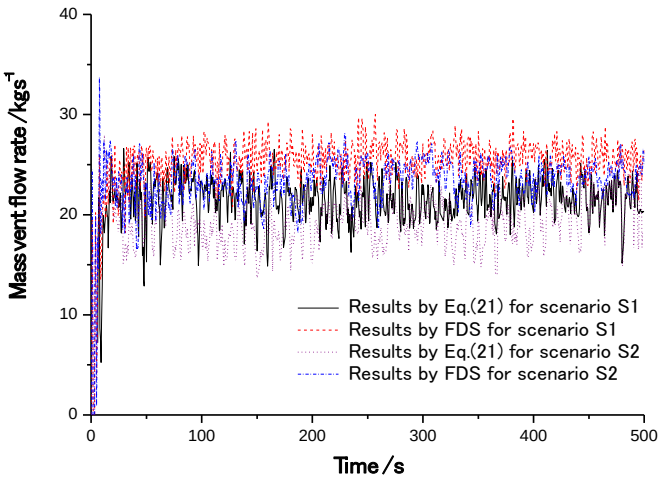

(c) Numerical mass vent flow rate across the ceiling vent

Figure 7: Predicted results under a 5 MW fire and wind speed of 5 ms^{-1} in scenarios S1 and S2

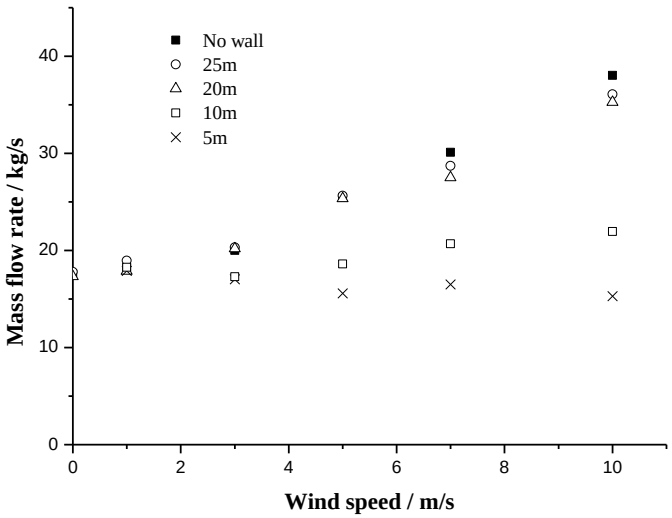

Figure 8: Variation of the vent mass flow rates with the distance of the vertical wall to the building and external wind speed (Q = 3 MW)

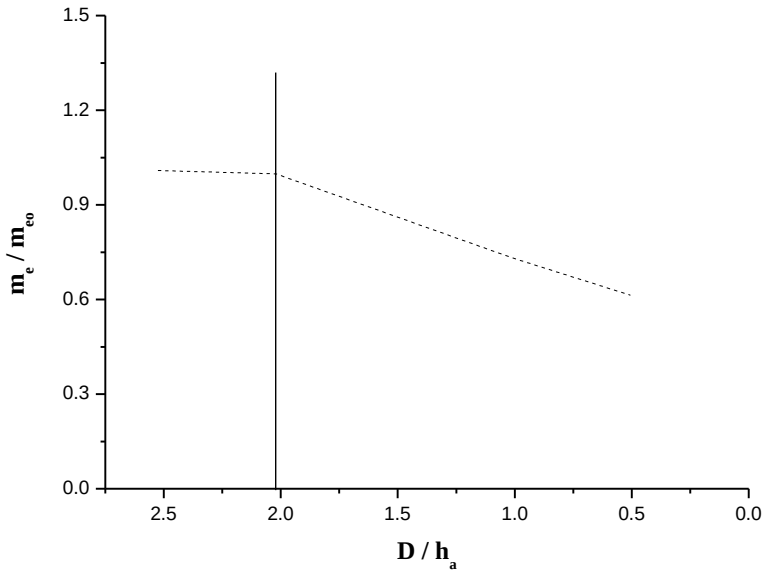

Figure 9: Variation of m_e / m_{eo} with dimensionless distance away from the adjacent vertical wall